HHS Public Access

Author manuscript

Pediatr Neurol. Author manuscript; available in PMC 2020 January 01.

Published in final edited form as:

Pediatr Neurol. 2019 January ; 90: 24–30. doi:10.1016/j.pediatrneurol.2018.10.005.

Longitudinal effects of everolimus on white matter diffusion in Tuberous Sclerosis Complex

Jurriaan M. Peters, MD, PhD[1,2,3], **Anna Prohl, BA**[2], **Kush Kapur, PhD**[3], **Audrey Nath, MD, PhD**[4], **Benoit Scherrer, PhD**[3], **Sean Clancy, BA**[3], **Sanjay P. Prabhu, MBBS**[3], **Mustafa Sahin, MD, PhD**[2], **David Neal Franz, MD, PhD**[4], **Simon K. Warfield, PhD**[3], and **Darcy A Krueger, MD, PhD**[4]

[1]Division of Epilepsy and Clinical Neurophysiology, Boston, MA 02115

[2]Translational Neuroscience Center, Department of Neurology, Boston Children's Hospital and Harvard Medical School, Boston, MA 02115

[3]Computational Radiology Laboratory, Department of Radiology, Boston Children's Hospital and Harvard Medical School, Boston, MA 02115

[4]Department of Neurology, Cincinnati Children's Hospital Medical Center, Cincinnati, OH.

Abstract

Objective: To study longitudinal effects of everolimus, an inhibitor of the mechanistic target of rapamycin (mTOR), on callosal white matter diffusion tensor imaging (DTI) in patients with tuberous sclerosis complex (TSC).

Methods: Serial imaging data spanning 9 years was used from the open label, Phase I/II trial (NCT00411619) and open-ended extension phase of everolimus for the treatment of subependymal giant cell astrocytoma (SEGA) associated with TSC. From 28 patients treated with everolimus, and 25 untreated control patients, 481 MRI scans were available. Rigorous quality control resulted in omission of all scans with DWI data in <15 directions or >8 artifacted volumes, and all post-surgical scans. We applied a linear mixed-effects model to the remaining 125 scans

Department of Correspondence: Jurriaan M. Peters, MD, PhD. Division of Epilepsy and Clinical Neurophysiology, Boston Children's Hospital. 300 Longwood Ave – Fegan 9, Boston, MA 02115, USA. Tel +1 617 355 5606 Fax +1 617 730 0463 jurriaan.peters@childrens.harvard.edu.

Disclosures

DF and DK led the original Phase I/II trial (NCT00411619) and the open-ended extension phase, from which this data was derived, funded by Novartis. JP, MS, DF and DK have participated in the Novartis EXIST-III trial (NCT01713946), although that data was not used for this study.

DK has received consulting and speaking fees and travel expenses from Novartis and Upsher-Smith Pharmaceuticals. In addition, he has received research support from Novartis Pharmaceuticals.

DF discloses research support and a consulting role with Novartis, and a consulting role with Aeonian Pharmaceuticals. MS reports grant support from Novartis, Roche, Pfizer, Ipsen, LAM Therapeutics and Quandrant Biosciences. He has served on Scientific Advisory Boards for Sage, Roche and Takeda.

Novartis did not provide funding of any sort, or editorial assistance of any kind, to this work. In addition, all clinical data and relevant images were available to the authors for review and processing.

(17 treated, 24 controls) for longitudinal analysis of each DTI metric of manually drawn callosal regions of interest.

Results: On a population level, mTOR inhibition was associated with a decrease in mean diffusivity. In addition, in treated patients only, a decrease of radial diffusivity was observed; in untreated patients only, an increase of axial diffusivity was seen. In patients below age 10, effect-sizes were consistently greater, and longer treatment was associated with greater rate of diffusion change. There was no correlation between DTI metrics and reduction of SEGA volume, or everolimus serum levels.

Conclusion: Effects from mTOR overactivity on white matter microstructural integrity in TSC were modified through pharmacological inhibition of mTOR. These changes sustained over time, were greater with longer treatment and in younger patients during a time of rapid white matter maturation.

Keywords

children; tuberous sclerosis complex; diffusion tensor imaging; mechanistic target of rapamycin; mTOR

Introduction

Tuberous sclerosis complex (TSC) is a genetic autosomal dominant neurocutaneous disorder related to pathogenic variants in the *TSC1/TSC2* genes with subsequent overactivity of the mechanistic target of rapamycin (mTOR) pathway. Neurological symptoms include epilepsy, intellectual disability, behavioral dysregulation, autism spectrum disorder and growth of deep, potentially obstructive lesions called subependymal giant cell astrocytoma (SEGA). The clinical phenotype is highly variable and unpredictable, and worse neurodevelopmental outcomes are seen with early and severe epilepsy[1].

Biomarkers are needed to identify high-risk patients, for clinical trials of early and pre-emptive seizure control and for mitigation of early autistic symptoms through intense behavioral programs[2,3]. A biomarker of neurological disease severity in TSC should be accurate and reproducible, and ideally reflect the biological process, pathogenic process, or therapeutic intervention.

Diffusion tensor imaging (DTI) of the white matter is potentially such a biomarker, as DTI metrics of various tracts correlate with autism spectrum disorder, refractory epilepsy and intellectual disability[4]. Microstructural integrity of the corpus callosum reflects the overall neurological disease burden but is not specific to any symptom.

mTOR inhibitors dampen the overactive mTOR pathway, two steps downstream from the malfunctioning TSC1/2 protein complex in TSC. Everolimus (Afinitor/Votubia, Novartis, East Hanover, NJ) is FDA-approved for treatment of renal angiomyolipomas, subependymal giant cell astrocytoma (SEGA) and recently for the adjunctive treatment of refractory seizures in TSC[5]. The Phase I/II trial demonstrated a significant reduction in SEGA volume, and the long-term efficacy and safety data of this same cohort exhibited a sustained effect with continuing reduction in SEGA size[6].

In addition to SEGA volume reduction, we previously reported altered DTI measurements after 12–18 months on treatment. In a group of 21 treated patients, fractional anisotropy (FA) increased and mean diffusivity (MD) decreased in the corpus callosum and other regions of interest (ROIs), while no such change was seen in a group of age- and gender-matched controls with TSC but no treatment[7].

In a recent Phase III trial, longer exposure to everolimus was associated with an incremental effect on seizure reduction[5], and a better response was seen with younger age[8]. We hypothesized that treatment effects on white matter DTI metrics would sustain also. To test this hypothesis, we expanded on our previous work and analyzed the longitudinal diffusion imaging data from the same patients in the Phase I/II trial and open-ended extension phase[6, 7]. In addition, we examined effects from age, duration of treatment, everolimus serum levels, and percent SEGA volume reduction.

Methods

Study Design

This study included participants enrolled in an open label, Phase I/II trial (NCT00411619) and open ended extension phase of everolimus for the treatment of SEGAs associated with TSC, conducted at Cincinnati Children's Hospital Medical Center. Twenty-eight TSC patients older than age 3 were enrolled. All patients were diagnosed following clinical and/or genetic criteria of TSC, and had serial growth of SEGA on 2 or more consecutive MRIs. Treatment protocol, serum and MRI monitoring has been reported previously[9, 10]. Target everolimus concentrations were 5–15 ng/mL. SEGA and hydrocephalus were monitored with volumetric MRI at 3, 6 and 12 months after initiation of everolimus, and every 6 months thereafter unless clinical course dictated otherwise.

The control group included imaging data from 25 age- and gender matched patients with TSC, identified through a database from the CCHMC TSC clinic. Participants met clinical and/or genetic criteria of TSC and had no history of exposure to medication affecting the mTOR pathway. Scans were obtained per TSC clinical surveillance guidelines[11, 12] and not part of the Phase I/II trial; thus, scan intervals were not as frequent but the acquisition protocol was similar.

Informed consent was obtained from adult patients, and from parents or guardians for patient under 18 years of age. Assent was provided by patients when able per institutional requirements. The CCHMC institutional review board approved the protocol.

MRI Acquisition

MRI scans were acquired on 1.5T GE Signa HDxt, 1.5T GE Signa Excite, 3T GE Discovery, 3T Philips Achieva and 3T Philips Ingenia scanners over a course of 9 years (May 2006 - June 2015). The imaging protocol included: sagital MPRAGE, T2w TSE, and 15 diffusion weighted echoplanar images acquired in the axial plane (b-value 1,000 s/mm^2, repetition time/echo time 12,000/81–101, field of view 384×384 mm, 3 mm^3) covering the entire brain. Note that DWI was not part of the formal Phase I/II study protocol, and that during the course of the open-ended extension phase, MRI scanners underwent upgrades and scans

were performed at local hospitals and transmitted to CCHMC, resulting in some MR protocol variability and warranting extensive quality control procedures (see below).

MRI Quality Assurance

Four hundred eighty-one scans from 28 patients and 25 controls were available for analysis. T1w, T2w, and all DWI volumes were reviewed for artifact (motion, susceptibility, scanner-related) by expert raters. Scans were excluded as follows: no DWI acquired (n=54), fewer than 15 DWI directions acquired (n=68), greater than 8 DWI volumes of artifact due to patient motion, magnetic susceptibility, severe echo planar imaging (EPI) distortion, or hardware induced artifact (n=181), and prior neurosurgery (n=53) (Figure 1).

After curation of the MRI dataset, 17 patients on everolimus were included with 76 MRIs on 3 different scanners: 3T Phillips Achieva (n=8), 1.5T GE Excite (n=7), and 1.5 GE Signa HDxt (n=61). 24 control patients had 49 MRIs of sufficient quality, acquired on 5 different scanners: 3T Phillips Achieva (n=3), 1.5T GE Excite (n=8), 1.5 GE Signa HDxt (n=36), 3T GE Discovery MR750w (n=1), 1.5T Phillips Ingenia (n=1) (Table 1).

MRI Processing

All MRI processing and analyses were performed using the Computational Radiology Kit (http://crl.med.harvard.edu). For each scan, the T2w was aligned to the T1w image and the intracranial cavity was segmented using a previously validated multispectral method[13]. DWI data were screened for intra-volume motion and scanner artifact by expert raters, and artifacted volumes were removed. Inter-volume motion correction was performed via affine registration of each DWI volume to the mean b=0 s/mm^2 image. DWI were upsampled to the T1w image and skull stripped with the intracranial cavity segmentation. A single tensor diffusion model was estimated using robust least squares in each brain voxel from which fractional anisotropy ($FA=3Var(\lambda)/(\lambda^2_1 + \lambda^2_2 + \lambda^2_3)^{1/2}$), mean diffusivity ($MD=(\lambda_1 + \lambda_2 + \lambda_3)/3$, radial diffusivity ($RD=(\lambda_2 + \lambda_3)/2$), and axial diffusivity = (λ_1) were computed.

Callosal ROIs were manually drawn in 5 parasagittal planes in each scan, with ITK-SNAP 2.0 (www.itksnap.org). Mean values of FA, MD, RD, and AD were measured in each ROI.

Statistical analysis

Statistical analyses were performed using software R (CRAN, Vienna, Austria, www.R-project.org) and SAS Version 9.4 (SAS Institute, Inc Cary NC). Longitudinal analysis of each DTI metric for the callosal ROI was done using a linear mixed-effects model. The model consisted of intercept, slope of log age at baseline, slope of within-subject (WS) effect of log age, and interaction of treatment status (everolimus vs. controls) with the WS effect of log age as fixed effects. The random intercept and slope terms were included to account for WS correlations and between subject variability.

Likelihood ratio tests were used to determine the significance of variance covariance parameters of the random-effects among nested models. Final model selection was performed using Akaike Information Criterion (AIC). All fixed-effects were retained in the final models irrespective of their statistical significance to understand the relationship

between DTI metrics and treatment status. For the analysis, DTI FA was multiplied by a scale factor of 10, and DTI MD, RD, and AD were multiplied scaled by a scale factor of 1,000. Finally, missing data were not imputed and all the available measurements were included in the analysis under the missing-at-random assumption.

Given the steep developmental trajectory of diffusion metrics before approximately age 10[14, 15], and a higher response rates of seizures in younger patients[8], we analyzed the data separately for those <10 years of age. Duration of treatment (at time of each scan), mean everolimus levels (over the full course of treatment) and maximum percentage of SEGA volume decrease were introduced in the model as continuous variables.

Results

Patients

Demographic and clinical data of included patients are shown in Table 1. While the Phase I/II trial and open-ended extension phase contained 28 patients, and we previously reported on diffusion imaging findings in 21 of these[7], in the current work the quality of the data limited the analysis to 17 patients. There were more males in the treated group, and age was higher in the untreated group. The total number of scans per patient and interval between scans was higher in the treated group. Mean duration of treatment was 3.5 years. The mean serum level (5.8 ng/mL), and mean maximum SEGA volume decrease (50.8%) showed little variation for the length of the study across the majority of patients receiving treatment.

DTI

Table 2 summarizes the findings in our model, and Figure 2 displays longitudinal changes in the subgroup of patients below 10 years of age. Of importance, the model assesses for mean changes on a population level, compared to controls.

In all ages combined, and in the subgroup below 10 years of age, FA increased in both treated and untreated patients. This age-related FA increase occurred at the same rate in treated and untreated patients.

Across all ages, and in the younger patients, no changes in MD with age were seen in the untreated patients. The MD decreased, however, in the treated patients across all ages, and in the younger subgroup. As a result, this longitudinal MD change was significantly different between treated vs. untreated patients.

In all patients, the RD decreased only in the treated patients; this was also seen in the subgroup of patients below 10 years old. The RD in the untreated patients did not significantly change. The RD changes, however, were not different between treated vs. untreated patients.

In all patients, as well in the younger subgroup, the AD in the untreated patients increased. It did not change in treated patients. For all patients and in the younger patient subgroup, the AD changes over time were significantly different in treated vs. untreated subjects.

Treatment variables

With respect to (log) age, the linear rate of FA change was not associated with duration of everolimus treatment when evaluated for all patients. In the younger subgroup, however, steeper increases were seen with longer treatment ($p = 0.024$).

For MD and RD a similar but inverse association was seen between rate of change and duration of treatment ($p = 0.0321$ and $p = 0.014$, respectively). This association was also present in the younger subgroup ($p = 0.039$ and 0.0205, respectively).

Longitudinal DTI metrics were not statistically associated with the maximum SEGA volume decrease, or with mean serum levels (Supplementary table 1).

Discussion

We demonstrated that pharmacological inhibition of mTOR was associated with a decrease in MD which was not seen in untreated patients with TSC. In treated patients only, a decrease of RD was observed; in untreated patients only, an increase of AD was seen. Effect-sizes were consistently greater in the younger subpopulation. Through rigorous quality control of heterogeneous longitudinal imaging data, our previous findings confirmed and expanded our earlier study suggesting genetic effects from mTOR overactivation on the white matter can be modified[7].

In the EXIST-3 trial of adjunctive everolimus for refractory focal-onset seizures in TSC, further seizure reduction was seen with ongoing treatment[5] and efficacy was higher in younger patients[8]. Similarly, in our longitudinal imaging study, diffusion changes were sustained, steeper over time with ongoing treatment, and more evident in patients under 10 years of age. A dose-response effect, as seen in the EXIST-3 trial in which everolimus was stratified by design into lower and higher target dosing ranges, could not be established in this study. This is likely due to relatively homogenous everolimus serum levels in our cohort in which all subjects belonged to a single targeted dosing range. We continued to see no association with percent SEGA volume change, as previously reported[7].

Previously reported lower FA and higher MD in the callosal white matter of patients with TSC as compared to healthy controls were mainly driven by a increases in RD[16–18], or in both RD and AD[4, 15].

For RD, a potential explanation could be qualitative changes in myelination. In the white matter of a neuronal *Tsc1* knockout model of TSC, hypomyelination was rescued by mTOR inhibition[19]. In a oligodendrocyte precursor *Tsc2*-knockout mouse model, diffuse hypomyelination was associated with decreased RD[20]. In pediatric patients with TSC, ex-vivo diffusion imaging of resection specimen from epilepsy surgery revealed consistent correlations between myelin content and MD (unpublished data).

Alternatively, imaging and neuropathogical studies have demonstrated extensive heterotopic neurons and cells of mixed glial and neuronal lineage throughout the white matter[14, 21]. A reduction in volume or morphology of such cells through mTOR inhibition could lead to increased axonal packing, and a subsequent lower RD.

The AD increased in untreated patients AD over time, which could be due to a increases in axon diameter, as seen on electron microscopy in *Tsc1* neuronal knockout mice[22]. This increase, however, is opposite of a typical age-effect previously reported[14]. No such changes of AD were seen in the treatment group, possibly related to inhibition of mTOR.

Two indirect mechanisms could also be responsible for the observed changes in diffusivity. First, impending hydrocephalus or altered ventricular morphology from elevated cerebrospinal fluid pressure could increase extracellular water in the periventricular white matter. Transependymal flow, however, was not seen on conventional imaging and there was again no correlation of mean diffusion metrics with reduction in SEGA volume. In addition, we have previously demonstrated similar diffusion changes in tracts more remote from the ventricles[7].

Second, refractory epilepsy as a co-morbid condition in TSC is associated with a greater increase in diffusivity[4, 23], and longitudinal effects on diffusion have also been reported[24]. Reduced seizures were seen in the treatment group[10], potentially resulting in altered diffusivity as compared to untreated patients. Seizure frequency, however, was assessed via parental report (and video-EEG in some) and the study design did not allow for a formal prospective analysis[7].

Limitations include the low number of subjects and only one experienced collaborator manually marked the ROIs. This work is technically limited by a variable quality of the imaging, warranting a meticulous process of data review, and either salvaging or omitting bad scans. Nonetheless, the data remained noisy with a risk of both type I and type II errors. It's possible that the lack of FA changes is due to decreased robustness of FA as compared to MD with regards to motion artifact[25], and also explains why generation of callosal tractography data was unsatisfactory. The inclusion of poor quality data can severely affect findings; in our study, more MRI volumes needed removal in the treatment group (data on file), potentially biasing results. On the other hand, reliability of DTI data can be improved through implementation of stringent quality control measures[26].

In summary, callosal DTI metrics reflect the neurological disease burden in TSC[4], and the current work demonstrates that these metrics respond to targeted treatment. To truly study the effects of mTOR inhibitors on white matter diffusion in the context of biomarker discovery, however, a proper multicenter prospective data collection effort is needed. Such a study would include strict acquisition protocols, centralized quality control with periodic calibration of both phantom and human data across sites.

Acknowledgements

JP, SC, MS, SW are supported by NIH R01 NS079788 and U01 NS082320 grants. DK is supported by NIH U01-NS082320, U54-NS092090 and U01-NS092595. SP is supported by the Department of Defense W81XWH-11-1-0365 and NIH U01 NS082320 grants. MS is additionally supported by an NIH U54 HD090255 grant and the Boston Children's Hospital Translational Research Program. The Developmental Synaptopathies Consortium (U54 NS092090) is part of the NCATS Rare Diseases Clinical Research Network (RDCRN). RDCRN is an initiative of the Office of Rare Diseases Research (ORDR), NCATS, funded through collaboration between NCATS, NIMH, NINDS, and NICHD.

References

1. Capal JK, Bernardino-Cuesta B, Horn PS, et al. Influence of seizures on early development in tuberous sclerosis complex. Epilepsy Behav 2017;70:245–252. [PubMed: 28457992]
2. Goods KS, Ishijima E, Chang YC, Kasari C. Preschool based JASPER intervention in minimally verbal children with autism: pilot RCT. J Autism Dev Disord 2013;43:1050–1056. [PubMed: 22965298]
3. Kasari C, Gulsrud A, Paparella T, Hellemann G, Berry K. Randomized comparative efficacy study of parent-mediated interventions for toddlers with autism. Journal of consulting and clinical psychology 2015;83:554–563. [PubMed: 25822242]
4. Baumer FM, Peters JM, Clancy S, et al. Corpus callosum white matter diffusivity reflects cumulative neurological comorbidity in Tuberous Sclerosis Complex. Cereb Cortex 2017;in press.
5. French JA, Lawson JA, Yapici Z, et al. Adjunctive everolimus therapy for treatment-resistant focal-onset seizures associated with tuberous sclerosis (EXIST-3): a phase 3, randomised, double-blind, placebocontrolled study. Lancet 2016;388:2153–2163. [PubMed: 27613521]
6. Krueger DA, Care MM, Agricola K, Tudor C, Mays M, Franz DN. Everolimus long-term safety and efficacy in subependymal giant cell astrocytoma. Neurology 2013;80:574–580. [PubMed: 23325902]
7. Tillema JM, Leach JL, Krueger DA, Franz DN. Everolimus alters white matter diffusion in tuberous sclerosis complex. Neurology 2012;78:526–531. [PubMed: 22262746]
8. French JA, Curatolo P, Lawson JA, et al. Adjunctive Everolimus in Patients with Treatment-Refractory Seizures Associated with Tuberous Sclerosis Complex (TSC): Analysis of Exposure-Efficacy and ExposureSafety Relationships in the Randomized, Phase 3, EXIST-3 trial American Academy of Neurology Annual Meeting. Los Angeles, CA 2018.
9. Franz DN, Agricola K, Mays M, et al. Everolimus for subependymal giant cell astrocytoma: 5-year final analysis. Ann Neurol 2015;78:929–938. [PubMed: 26381530]
10. Krueger DA, Care MM, Holland K, et al. Everolimus for subependymal giant-cell astrocytomas in tuberous sclerosis. N Engl J Med 2010;363:1801–1811. [PubMed: 21047224]
11. Krueger DA, Northrup H, International Tuberous Sclerosis Complex Consensus G. Tuberous sclerosis complex surveillance and management: recommendations of the 2012 International Tuberous Sclerosis Complex Consensus Conference. Pediatr Neurol 2013;49:255–265. [PubMed: 24053983]
12. Roach ES, DiMario FJ, Kandt RS, Northrup H. Tuberous Sclerosis Consensus Conference: recommendations for diagnostic evaluation. National Tuberous Sclerosis Association. J Child Neurol 1999;14:401–407. [PubMed: 10385849]
13. Grau V, Mewes AU, Alcaniz M, Kikinis R, Warfield SK. Improved watershed transform for medical image segmentation using prior information. IEEE Trans Med Imaging 2004;23:447–458. [PubMed: 15084070]
14. Peters JM, Prohl AK, Tomas-Fernandez XK, et al. Tubers are neither static nor discrete: Evidence from serial diffusion tensor imaging. Neurology 2015;85:1536–1545. [PubMed: 26432846]
15. Peters JM, Sahin M, Vogel-Farley VK, et al. Loss of white matter microstructural integrity is associated with adverse neurological outcome in tuberous sclerosis complex. Acad Radiol 2012;19:17–25. [PubMed: 22142677]
16. Makki MI, Chugani DC, Janisse J, Chugani HT. Characteristics of abnormal diffusivity in normal-appearing white matter investigated with diffusion tensor MR imaging in tuberous sclerosis complex. AJNR Am J Neuroradiol 2007;28:1662–1667. [PubMed: 17893226]
17. Simao G, Raybaud C, Chuang S, Go C, Snead OC, Widjaja E. Diffusion tensor imaging of commissural and projection white matter in tuberous sclerosis complex and correlation with tuber load. AJNR Am J Neuroradiol 2010;31:1273–1277. [PubMed: 20203114]
18. Krishnan ML, Commowick O, Jeste SS, et al. Diffusion features of white matter in tuberous sclerosis with tractography. Pediatr Neurol 2010;42:101–106. [PubMed: 20117745]
19. Meikle L, Talos DM, Onda H, et al. A mouse model of tuberous sclerosis: neuronal loss of Tsc1 causes dysplastic and ectopic neurons, reduced myelination, seizure activity, and limited survival. J Neurosci 2007;27:5546–5558. [PubMed: 17522300]

20. Carson RP, Kelm ND, West KL, et al. Hypomyelination following deletion of Tsc2 in oligodendrocyte precursors. Annals of clinical and translational neurology 2015;2:1041–1054. [PubMed: 26734657]

21. Marcotte L, Aronica E, Baybis M, Crino PB. Cytoarchitectural alterations are widespread in cerebral cortex in tuberous sclerosis complex. Acta Neuropathol 2012;123:685–693. [PubMed: 22327361]

22. Ercan E, Han JM, Di Nardo A, et al. Neuronal CTGF/CCN2 negatively regulates myelination in a mouse model of tuberous sclerosis complex. The Journal of experimental medicine 2017;214:681–697. [PubMed: 28183733]

23. Moavero R, Napolitano A, Cusmai R, et al. White matter disruption is associated with persistent seizures in tuberous sclerosis complex. Epilepsy Behav 2016;60:63–67. [PubMed: 27179194]

24. Baumer FM, Song JW, Mitchell PD, et al. Longitudinal changes in diffusion properties in white matter pathways of children with tuberous sclerosis complex. Pediatr Neurol 2015;52:615–623. [PubMed: 25817702]

25. Jiang S, Xue H, Counsell S, et al. Diffusion tensor imaging (DTI) of the brain in moving subjects: application to in-utero fetal and ex-utero studies. Magn Reson Med 2009;62:645–655. [PubMed: 19526505]

26. Roalf DR, Quarmley M, Elliott MA, et al. The impact of quality assurance assessment on diffusion tensor imaging outcomes in a large-scale population-based cohort. Neuroimage 2016;125:903–919. [PubMed: 26520775]

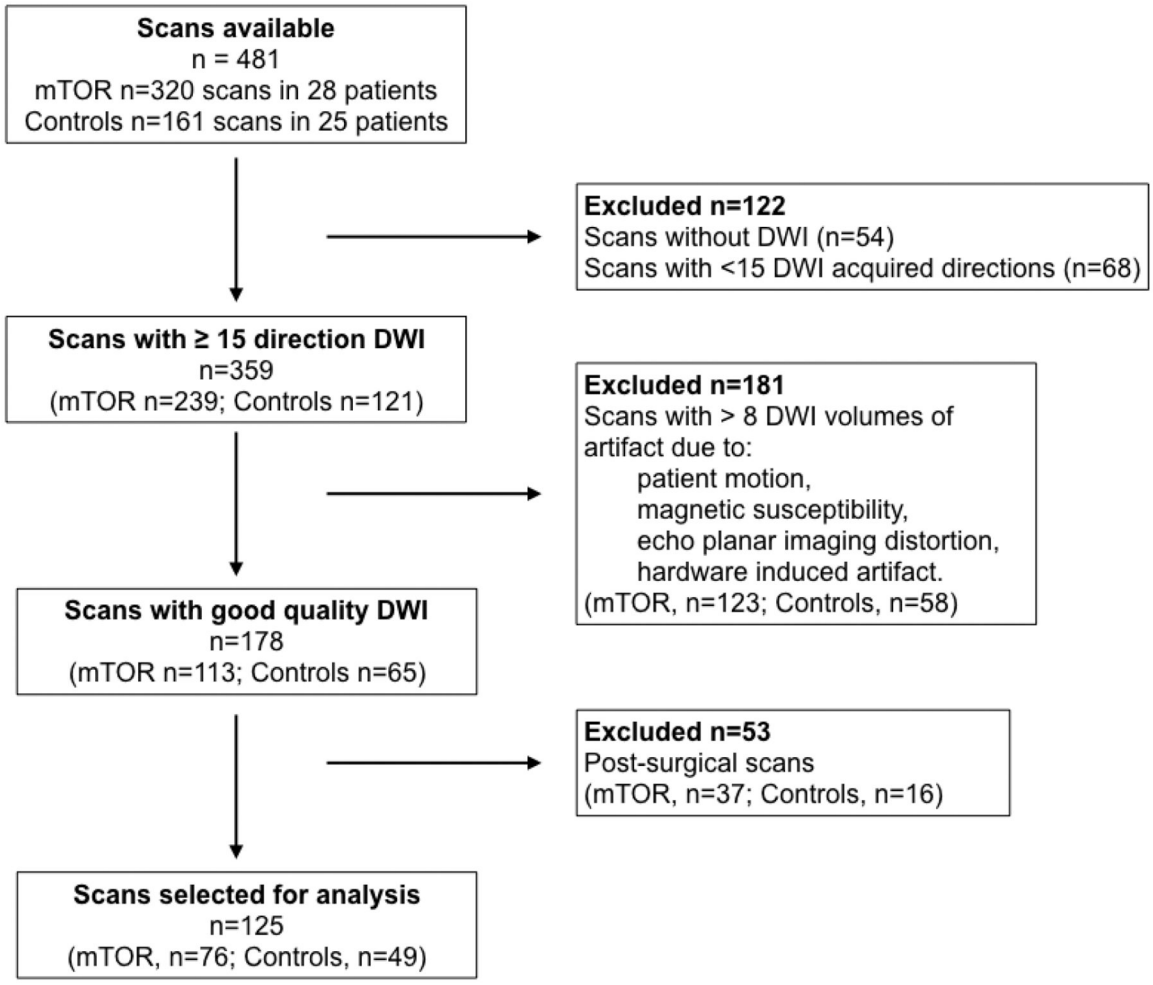

Figure 1. MRI quality assurance and data selection process.

Of the 481 scans available for all patients, 125 of 17 patients treated with everolimus and 24 intreated controls with TSC were included in data analysis after rigorous quality assurance. Scans with only some artifacted volumes could often be salvaged through reconstruction of the tensor data after omitting bad volumes. DWI diffusion-weighted imaging; mTOR mechanistic target of rapamycin

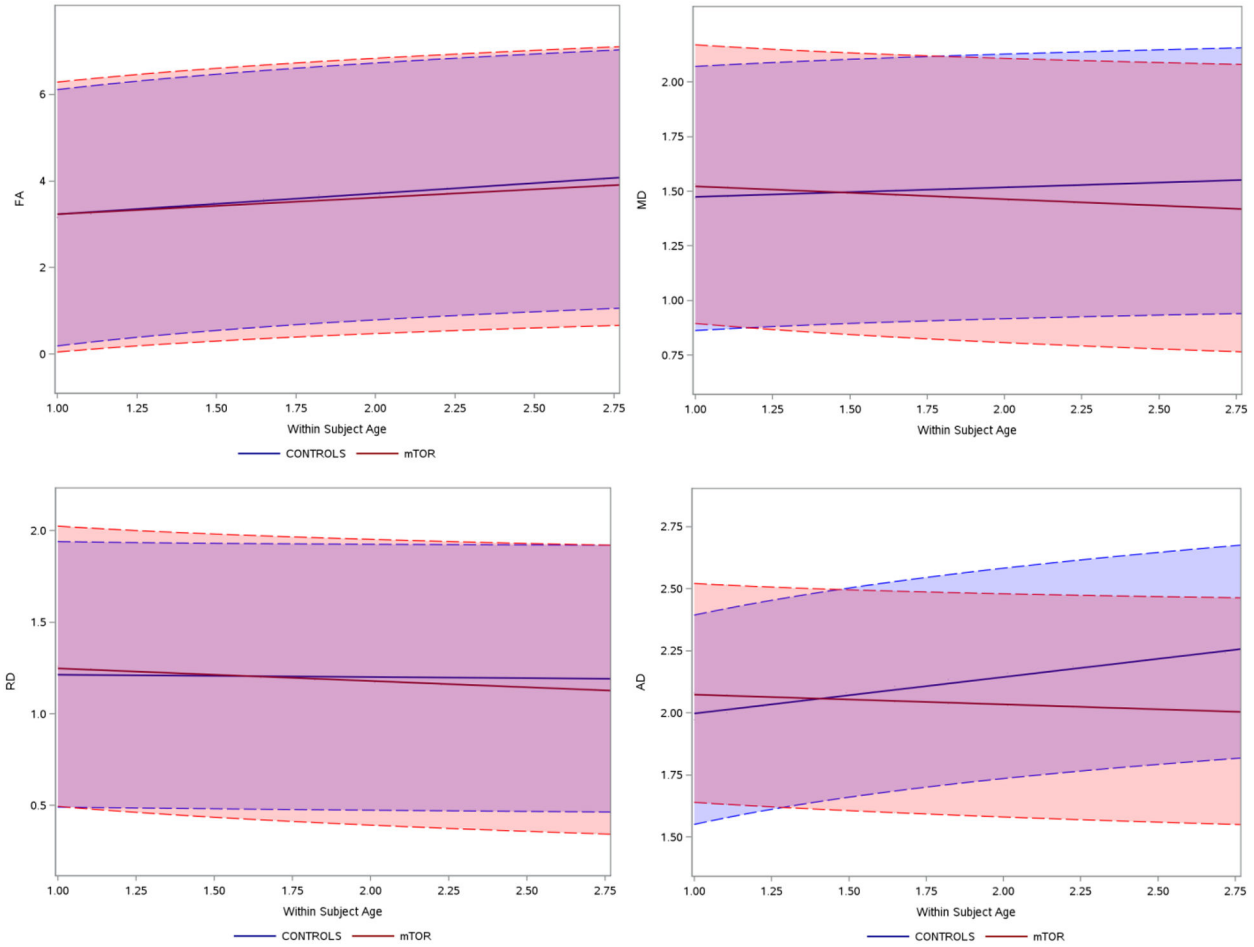

Figure 2. Longitudinal diffusion changes, treated (mTOR) vs. untreated, ≤ 10 years.

Diffusion changes over time in treated group (mTOR, red) and untreated group (controls, blue). Orange and blue shaded areas indicate confidence intervals. On the y-axis, the four different DTI metrics. Note that for the analysis, FA was multiplied by a scale factor of 10, and DTI MD, RD, and AD were multiplied scaled by a scale factor of 1,000. On the x-axis, age is expressed a ratio: For example, if the subject is 2 years at time-point 1.0, the patient will be 5 years old at time-point 2.5. FA fractional anisotropy; MD mean diffusivity; RD radial diffusivity; AD axial diffusivity

Table 1:

Patient demographics, MRI data

	≤10 years		All	
	mTOR	**Controls**	**mTOR**	**Controls**
Number of participants	8	14	17	24
Sex (%male)	75	50	71	54
Age, mean (SD) (years)	9.1 (1.8)	7.8 (2.2)	12.8 (4.7)	14.7 (9.0)
Age range (years)	[3.5, 10.87]	[37, 107]	[3.5, 25.7]	[3.7, 44.3]
Duration of treatment, mean (SD) (years)*	3.4 (1.6)	-	3.5 (2.3)	-
Serum levels, mean (SD) (ng/mL)	5.7 (1.9)	-	5.8 (2.6)	-
% Maximum SEGA volume decrease, mean(SD)	50.8 (20.1)	-	50.8 (19.6)	-
Number of scans	31	18	76	49
Number of scans per participant, mean (SD)	4.1 (2.2)	1.3 (0.6)	4.5 (3.0)	2.0 (1.04)
Number of DWI volumes removed, mean (SD)	0.4 (1.2)	0.2 (0.7)	0.3 (0.9)	0.4 (1.3)
Number of participants with 1 scan	1 (12.5%)	11 (79%)	5 (29%)	7 (29%)
Number of participants with 2 scans	1 (12.5%)	2 (14%)	1 (6%)	13 (55%)
Number of participants with 3 scans	1 (12.5%)	1 (7%)	2 (12%)	1 (4%)
Number of participants with 4 scans	1 (12.5%)	0	0	2 (8%)
Number of participants with 5 or more	4 (50%)	0	9 (53%)	1 (4%)

mTOR patients on everolimus, an inhibitor of the mechanistic target of rapamycin; SEGA subependymal giant cell astrocytoma; DWI diffusion weighted imaging

Table 2:

Longitudinal effects on diffusion metrics in treated and untreated patients with Tuberous Sclerosis Complex

		≤10 years			All		
	Within subject age effect	**Estimate**	**95% Confidence interval**	**p-value**	**Estimate**	**95% confidence interval**	**p-value**
FA	Controls	0.8797	(0.368,1.392)	0.0012	0.647	(0.181,1.114)	0.007
	Patients on mTOR-inhibitor	0.7037	(0.241,1.167)	0.0038	0.654	(0.210,1.0987)	0.0044
	mTOR vs. Controls	−0.1759	(−0.866,0.514)	0.61	0.00682	(−0.634,0.650)	0.983
MD	Controls	0.0799	(−0.00895,0.169)	0.0768	0.0549	(−0.0191,0.129)	0.144
	Patients on mTOR-inhibitor	−0.108	(−0.188, −0.0277)	0.0096	−0.092	(−0.163,0.0218)	0.0108
	mTOR vs. Controls	−0.188	(−0.307, −0.0681)	0.0029	−0.147	(−0.249,−0.0452)	0.0052
RD	Controls	−0.0228	(−0.124,0.0783)	0.652	−0.0177	(−0.101,0.0659)	0.675
	Patients on mTOR-inhibitor	−0.126	(−0.217, −0.0344)	0.0081	−0.113	(−0.193,−0.0335)	0.0059
	mTOR vs. Controls	−0.103	(−0.239,0.0334)	0.135	−0.0953	(−0.211,0.0200)	0.104
AD	Controls	0.270	(0.162,0.378)	<.000	0.172	(0.0706,0.273)	0.0011
	Patients on mTOR-inhibitor	−0.0722	(−0.171,0.0262)	0.146	−0.0475	(−0.145,0.0499)	0.335
	mTOR vs. Controls	−0.342	(−0.488, −0.196)	<.0001	−0.219	(−0.359,−0.0796)	0.0024

FA fractional anisotropy; MD mean diffusivity; RD radial diffusivity; AD axial diffusivity; mTOR mechanistic target of rapamycin